RESEARCH ARTICLE

Pre-clinical and *In-silico* Analysis of the Augmentation of Dermal Regeneration by *Punica granatum* Linn Fruit Peel in Rats

Nimmy Varghese*, Prerana Shetty, Srusha Samani, Harsha Ashtekar

Nitte (Deemed to be University, NGSMIPS, Department of Pharmacology, Paneer, Deralakatte, Mangalore, India.

Received: 26th September, 2023; Revised: 04th October, 2023; Accepted: 09th November, 2023; Available Online: 25th December, 2023

ABSTRACT

Background: Pomegranate is a very delicious fruit having miraculous properties. It contains flavonoids, polyphenols, tannins, organic acid and water-soluble vitamins which contribute to a wide variety of pharmacological activity. We investigated the dermal regeneration bracing potential of the extract of *Punica granatum L.* dried peel. Also, computational studies for finding the phytochemicals responsible for the pharmacological activity was carried out.

Methods: Fruit peel of *P. granatum L.* was collected, dried and extracted by maceration using ethanol. We employed *in-vivo* screening methods *viz.* excision, incision and dead space wound repair animal models, silver sulfadiazine ointment was used as a reference standard.

Results: Dose-dependent and significant ($p < 0.05$) bracing of dermal regeneration was observed.

Keywords: *Punica granatum*, Wound healing models, *In-silico*.

International Journal of Drug Delivery Technology (2023); DOI: 10.25258/ijddt.13.4.45

How to cite this article: Varghese N, Shetty P, Samani S, Ashtekar H. Pre-clinical and *In-silico* Analysis of the Augmentation of Dermal Regeneration by *Punica granatum* Linn Fruit Peel in Rats. International Journal of Drug Delivery Technology. 2023;13(4):1412-1417.

Source of support: Nil.

Conflict of interest: None

INTRODUCTION

Dermal regeneration that happens after injury is the combination of regeneration and repair.[1,2] Our skin the primary defense system of our body protects and moderates all sort of insults whether it is mechanical, chemical or thermal kind.[3,4] Repair of breaches in the skin occurs by a well-organized sequential process that involves hemostasis, inflammation, proliferation and dermal remodeling resulting in architectural and physiological restoration.[1] Plants have been utilized all throughout human existence for the restoration and healing of wounds. In our laboratory investigation, we have found that the leaves of *Psidium guajava* extract could assist in wound healing in rats in various screening models of wound repair.[5,6]

Punica granatum L. contains pelargonin, protoxylocarpin A, B , C, D, and E, xylocarpin J, (9Z, 11E, 13Z)-octadecatrienoic acid, gedunin merulin A, B, C and D, steperoxide A. virtual screening of plant phytoconstituent for binding affinity with proteins involved in wound healing can assist in acquiring valuable information regarding the activity and pharmacokinetic profile of the plant bioactive.

The injuring process occurs in every organ and tissues of the body. Despite the fact that the procedure of mending is ceaseless, in light of its physiological process that is going on in and around encompassing tissues, the stages are divided as stage I-coagulation and hemostasis, followed by inflammation, proliferation as stage II, stage III, respectively and remodeling of the wound as stage IV.[7,8] A list of medicinal plants and their metabolites used for healing and wound repair is given by Sharma *et al*.[9] Pomegranate belongs to the family Lythraceae. The pomegranate is typically found in the northern hemisphere as well as the southern hemisphere from September to October and March to may, respectively. The primary qualitative study for phytoconstituents present in extract of pomegranate peel resulted in positive for flavonoids, phenols, tannins and terpenoids.[10] Attempts was made to investigate the capability of the concentrate of dried peel of *P. granatum* L. to assist the wound healing process using various experimental rat models.

MATERIALS AND METHODS

Animals and Treatment Protocol

Wistar rats of both sex of 180 to 200 g weight, 5 months old acquired from the animal repository of NGSMIPS, Mangalore, India. Study protocol was endorsed by IAEC committee of NGSMIPS. The rats were isolated and kept in proper cages independently. Standard dry pellet diet and water was given to animals. All the experiments were done in adherence to the CPCSEA guide lines. Five groups containing 6 animals each. Group I assigned as control and given no drug treatment. Group II animals received silver sulfadiazine ointment (5% w/w) applied topically on the wounded area and served as standard.

**Author for Correspondence: nimmychacko@nitte.edu.in*

Groups III to V given 100 (low), 200 (mid) and 400 (high) mg per kg of *P. granatum* fruit peel extract. The same treatment protocol was followed in all models of study.

Plant Material

The peel of *P. granatum L.* fruit was gathered the month of July. The plant was identified by Dr. K V Nagalaxmamma, Associate Professor, Botany Department, St. Aloysius school (Autonomous), Mangaluru. A sample of the fruit peel was submitted to the institutional herbarium and sample no. is 16PYO12.

Plant Extraction

The peels of pomegranate were gathered and cleaned, washed and shade dried. Dried peels were crushed and subjected to maceration with 90% of ethanol for 7 days with periodic stirring. Later it was filtered using a muslin cloth piece. The syrup acquired was evaporated till a dry concentrate was formed. The dull-coloured substance was stored in a desiccating chamber to prevent from moisture and degradataion.[11]

Primary Qualitative Bioactive Investigation

The *P. granatum L.* fruit peel ethanolic extract (PGEE) was subjected to preliminary evaluation for diverse bioactives such as alkaloids, carbohydrates, flavonoids, glycosides, phenol, proteins, saponins, steroids and terpenoids.[12]

Screening of Dermal Repair and Regeneration Potential of PGEE by *In-vivo* Technique

Wound healing excision animal model

Experimental rats were anesthetized using ketamine HCl (i.p. 10mg per kg B.W.). The dorsal surface was made hairless and circular area 4.9 cm^2 and depth of 0.2 cm was lacerated utilizing surgical instruments and the injured area was left open. Area of wound was analyzed on 1st to 14th days of time interval *via* outlining the wound on translucent sheet, area was calculated by means of 1 mm^2 graph sheet. Change in the area of wound noted and contraction evaluated by formula.[13-16]

% wound contraction = OWA-PWA/TWA *100

OWA - original wound area; PWA - Present wound area; TWA – total wound area

Incision wound healing animal model

A longitude para-vertebral 6 cm length cut was formed and then sutured. Further experimental animals were subjected to various treatments as mentioned earlier. On 8th day the sutures were opened. Further on 10th day skin breaking strength noted, with the help of a tensiometer.

Dead space wound healing animal model

The anesthetized rat was shaved on dorsal side and a wound was made, disinfected cotton pellets of weight 10 mg were embedded on the wounded surface of the rodent. The injury was left uncovered. On the tenth post-injuring day tissue collected for granulation on the embedded cotton pellets were collected and the damp mass of the tissue was assessed. These tissues was made dry and the dry mass was noted.[17-19]

Selection of Bioactive

The scaffold library reported plant bioactives were retrieved from ChEBI online database using the keyword "*P. granatum*". The bioactives were identified and the canonical smiles, Molecular weight, and molecular formula, PubChem ID were retrieved from PubChem database. The targets involved in the regulation of wound healing activity were retrieved from DISGENET database (C1851789). The bioactives were predicted for its protein targets by Swiss prediction online tool.[20-24]

Prediction of ADMET Property

The ADMET features of the bioactive of *P. granatum* were anticipated by ADMET sar 2.1online web server for predicting lipophilicity, bioavailability, pharmacokinetics, drug likeliness score and solubility parameter.[25-28]

In-silico Molecular Docking

Preparation of bioactive

The bioactive three-dimensional conformations were taken in the .sdf file format *via* Pub-chem database. Further these file is converted to PDB using biovia discovery studio visualizer. The energy of the compound is minimized in PyRX software and converted to pdbqt format.[29-32]

Receptor preparation

The target receptor was selected based on similarity using venny 2.1 from predicted disease genes and bioactive targeted protein. PDBID:1UBI was selected and saved in .pdb file. Then compound energy was minimized in PyRX software and converted to pdbqt format.[33-36]

Protein-ligand docking

Prepared protein target as well as bioactive compounds have been docked by autodock vina at PyRX version 0.8. The grid box size was kept at maximum with binding mode at 8 exhaustiveness. Further the lowest binding energy with the highest inter-molecular interfaces were carefully taken and investigated for protein-ligand interaction *via* biovia software.[37,38]

RESULTS AND DISCUSSION

Excision Wound Model

In the present study it was found that PGEE displayed a dose-reliant growth percentage of wound contraction (Figures 1-3). Animals treated with 400 mg/kg showed percentage wound

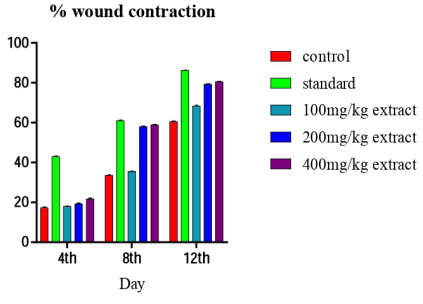

Figure 1: % wound contraction

Table 1: Effect of PGEE in excision wound model.

Parameter	*Day*	*Treatment groups*				
		Control	*STD*	*Low dose*	*Medium dose*	*High dose*
Wound area in mm^2	1^{st}	492.0 ± 0.8	491.3 ± 1.4	487.1 ± 1.6	488.8 ± 1.0	489.8 ± 1.8
	4^{th}	406.3 ± 2.0^{b}	279.6 ± 1.7^{a}	399.6 ± 0.9^{b}	393.6 ± $1.3^{a,b}$	382.6 ± $1.5^{a,b}$
	8^{th}	327.0 ± 1.4^{b}	191.3 ± 1.7^{a}	314.1 ± $1.6^{a,b}$	204.6 ± $1.0^{a,b}$	201.0 ± $1.7^{a,b}$
	12^{th}	194.0 ± 1.6^{b}	67.3 ± 0.8^{a}	153.5 ± $2.1^{a,b}$	100.8 ± $1.0^{a,b}$	95.1 ± $1.5^{a,b}$
	14^{th}	150.1 ± 3.3^{b}	35.5 ± 0.8^{a}	94.5 ± $1.7^{a,b}$	52.5 ± $1.6^{a,b}$	45.6 ± 1.3^{a}
% wound contraction	4^{th}	17.41 ± 0.2^{b}	43.08 ± 0.2^{a}	18.0 ± 0.2^{b}	19.3 ± $0.3^{a,b}$	21.8 ± $0.3^{a,b}$
	8^{th}	33.5 ± 0.17^{b}	61.06 ± 0.2^{a}	35.5 ± $0.2^{a,b}$	58.0 ± $0.2^{a,b}$	58.9 ± $0.2^{a,b}$
	12^{th}	60.5 ± 0.27^{b}	86.2 ± 0.13^{a}	68.4 ± $0.37^{a,b}$	79.3 ± $0.17^{a,b}$	80.5 ± $0.2^{a,b}$
	14^{th}	69.11 ± 0.11^{b}	92.7 ± 0.15^{a}	80.6 ± $0.30^{a,b}$	89.2 ± $0.33^{a,b}$	90.6 ± $0.2^{a,b}$

The values are represented as mean ± standard error of mean with $p < 0.05$ as statistically significant. a = $p<0.05$; b=$p<0.05$ compared to control and standard group respectively.

Table 2: Activity of wound healing of *P. granatum* L. ethanolic extract of fruit peel on incision model.

Parameter	*Treatment groups*				
	Control	*STD*	*Low dose*	*Medium dose*	*High dose*
Wound breaking strength	296.3 ± 10.2^{b}	431.6 ± 10.7^{a}	323.3 ± 4.4^{b}	381.6 ± $7.3^{a,b}$	422.5 ± 11.5^{a}

The values are represented as mean ± standard error of mean with $p < 0.05$ as statistically significant. a = $p<0.05$; b=$p<0.05$ compared to control and standard group respectively.

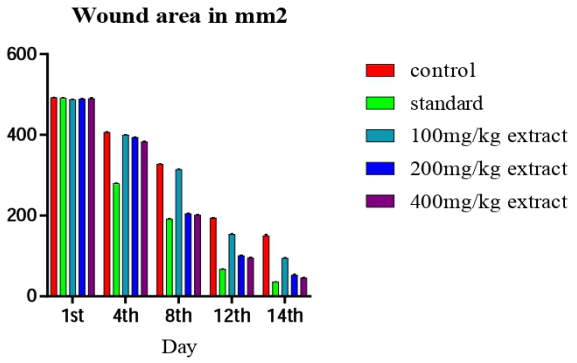

Figure 2: wound area in mm^2

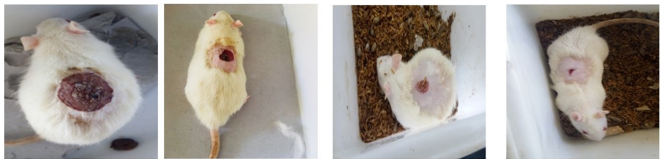

4^{th}DAY 8^{th}DAY 12^{th}DAY 15^{th}DAY

Figure 3: Excision-wound restorative action of (400mg/kg extract treated group on 4^{th}, 8^{th}, 12^{th}, 15^{th} day).

contraction of 90.6% and that of control animals 69.1% by the 16^{th} day. The standard drug-treated animals showed 92.7% wound contraction. The dose of 400 mg/kg and standard treatment displayed similar activity depicted in Table 1.

Incision Wound Healing

The wound-breaking capacity was evaluated in the experimental animal where the results shows that the control animal had wound-breaking strength less compared to standard drug treatment followed by 400 mg per kg drug then 200 and 100 mg/kg which indicate that at 400 mg per kg PGEE has given significant result compared to control animals which is depicted in Table 2 and Figure 4.

Dead Space Wound Healing

Dead space wound healing was calculated as wet weight and dry weight of the wound for standard was more compared to disease control followed by high dose, medium dose and low dose. Therefore, we observed that the high dose was significant against the control and standard group as depicted in Table 3.

Identification of Bioactives and Target involved in Wound Healing

Total 14 bioactives represented in Table 4 were identified from *P. granatum L.* and 19 genes associated with disease progression were retrieved from DisGeNET (C1851789) for wound healing with key name "wound healing". In this, total of 1.3% of the whole predicted genes from bioactives was present in the wound healing action (Figure 5 venny) and target measured was 1BUI for Pelargonin.

Figure 4: Incision wound healing model

Table 3: Effect of PGEE on dead space wound model

Parameter	*Control*	*STD*	*Low dose*	*Medium dose*	*High dose*
Wet weight	312 ± 1.06	482.8 ± 1.7	418.6 ± 1.45	436.3 ± 1.28	470.3 ± 0.6
Dry weight	91 ± 1.0	167 ± 2.0	113 ± 1.6	137 ± 1.6	151 ± 0.9

The values are represented as mean ± standard error of mean with $p < 0.05$ as statistically significant. a = $p<0.05$; b=$p<0.05$ compared to control and standard group respectively.

Table 4: Bioactives from *P. granatum L.*

Bioactives	*Molecular formula*	*Molecular weight*
Pelargonin	C27H31O15	595.53
protoxylocarpin A	C32H50O6	530.74
protoxylocarpin B	C32H50O6	530.74
protoxylocarpin C	C34H54O6	558.79
protoxylocarpin D	C31H48O6	516.71
protoxylocarpin E	C35H52O9	616.78
xylocarpin J	C32H42O9	570.67
(9Z,11E,13Z)-octadecatrienoic acid	C18H30O2	278.43
Gedunin	C28H34O7	482.57
Merulin A,	C14H22O4	254.32
Merulin B,	C15H24O5	284.35
Merulin C,	C15H22O5	282.33
Merulin D	C15H24O5	284.35
Steperoxide A	C14H22O4	254.32

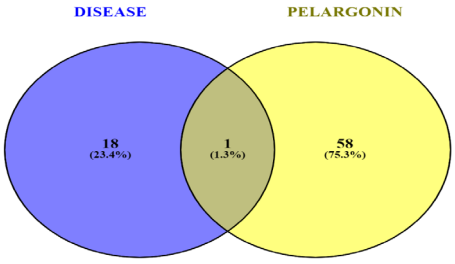

Figure 5: Venny diagram for selection of bioactives

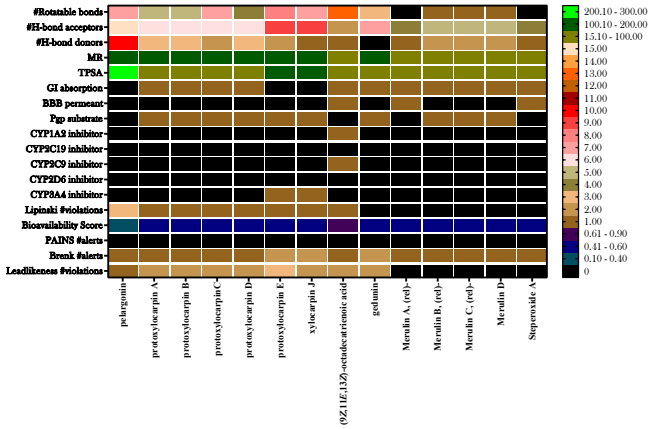

Figure 6: ADMET properties predicted by ADMET SAR2.0

ADMET Profile

The ADMET profile of the bioactives of *P. granatum* were predicted using ADMETSAR 2.0. to find the pharmacokinetics of bioactives and predict the variable parameters of the bioactives depicted in Figure 6.

Ames mutagenicity, oral toxicity, bioavailability

Bioactives were predicted to show negligible mutagenicity and they convert androgens into estrogens for gene expression. Acute oral toxicity[39] was predicted (Table 5), the study that evaluated oral absorption are predicted water solubility, CACO-2 cell penetrability to evaluate the non-active vehicle for gut barrier; compound OA, MA and SA showed permeability to gut blood border. The bioactives protoxylocarpin A, B, C, D, E, xylocarpin J, (9Z,11E,13Z) octadecatrienoic acid, gedunin, merulin A, B, C, D, steperoxide A can cross blood brain barrier and the bioactives pelargonin, protoxylocarpin A, B, C, D, E, xylocarpin, J have potential to cause drug-induced liver injury (DILI). Further, the CACO-2 predicted human intestinal absorption of (9Z,11E,13Z) octa-decatrienoic acid, merulin A, steperoxide A. All the bioactive bind to eastrogen receptor except merulin A, and steperoxide A. All bioactives except pelargonin are predicted to have human intestinal absorption. mMerulin A, and steperoxide A, possessed oral bioavailability.

Metabolism by Cytochrome Enzyme and Effect of Bioactives on Eye

(9Z,11E,13Z) Octadecatrienoic acid predicted to inhibit CYP1A2 whereas rest of the bioactives did not possess CYP2C19, CYP2C9, CYP2D6 inhibition as well as CYP2C9 and CYP2D6 substrate activity. The bioactives do not have tendency to cause eye irritation.

Toxicity and Detoxification

Bioactives were predicted negative for MATE 1 inhibition. pelargonin, merulin B; C; and D does not possess mitochondrial toxicity. Pelargonin is found to have micronuclear properties. xylocarpin J, merulin A, B, C, D; steperoxide A possess nephrotoxicity whereas (9Z,11E,13Z) octadecatrienoic acid shows reproductive toxicity and (9Z,11E,13Z) octadecatrienoic, pelargonin respiratory toxicity. The bioavives are predicted

Table 5: Acute toxicity category based on U.S. EPA6 study result

Acute toxicity	*oral (mg/kg)*
I Category	≤50
II Category	>50 ≤500
III Category	>500 ≤5000
IV Category	>5000

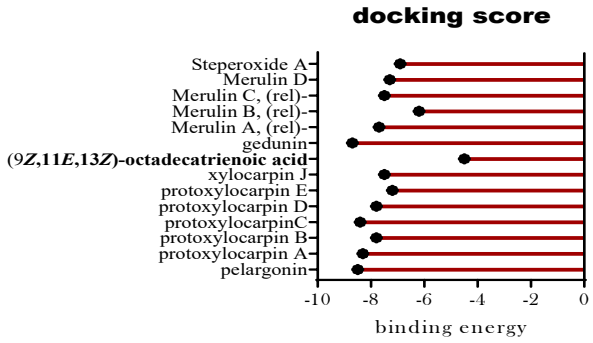

Figure 7: Docking scores with 1BUI

to have OATP1B1 inhibitory effect as OATP2B1 inhibitior show a negative prediction which implies to have poor oral absorption. The bioactive are predicted to possess OCT1 and OCT2 inhibitory effects which implies that they may detoxify exogenously administered compounds.

CNS effect

Also bioactives were predicted for p-glycoprotein inhibition and substrate. PPAR-gamma binding was positive for all the bioactives which implies a positive cognitive effect.

In-silico molecular docking

The compounds for docking was selected *via* chebi and targets were selected based on common targets from the disgenet for wound healing and swiss target-predicted proteins for bioactive 1BUI was selected as disease target for molecular docking. Gedunin podssess binding score of -8.7, followed by pelargonin (-8.5), protoxylocarpin C(-8.4), protoxylocarpin A(-8.3), protoxylocarpin B and protoxylocarpin D(-7.8), merulin A, (rel)-(-7.7), xylocarpin J and merulin C, (rel)-(-7.5), merulin D (-7.3), protoxylocarpin E (-7.2), Steperoxide A(-6.9), merulin B, (rel)-(-6.2) and lowest is (9*Z*,11*E*,13*Z*)-octadecatrienoic acid (-4.5) (Figure 7).

CONCLUSION

Dermal repair and regeneration involve a harmonized integration of events like cell immigration and multiplying and of extracellular matrix removal and remodeling. The study demonstrated that the PGEE has properties to assist the wound repair process mainly by free radical scavenging activity and anti-bacterial activity. In addition, tissue metalloproteinase inhibiting activity can promote collagen deposition and enable rapid maturation of granulation tissue. However, studies at molecular levels involving effect on chemical mediator levels and enzyme action are required to reveal the mechanism of action of *P. granatum* fruit peel as an agent that augments and brace the dermal regeneration and repair ability.

ACKNOWLEDGMENT

The authors express thankfulness to the authorities of Nitte (Deemed to be University) and the NGSMIPS, for supporting the facility to carry out the project.

REFERENCES

1. Tottoli EM, Dorati R, Genta I, Chiesa E, Pisani S, Conti B. Skin wound healing process and new emerging technologies for skin wound care and regeneration. Pharmaceutics. 2020;12(8):735.
2. Chiu A, Sharma D, Zhao F. Tissue engineering-based strategies for diabetic foot ulcer management. Advances in Wound Care. 2023;1;12(3):145-67.
3. Mazani M, Rezagholizadeh L, Shamsi S, Mahdavifard S, Ojarudi M, Salimnejad R, Salimi A. Protection of CCl4-induced hepatic and renal damage by linalool. Drug and Chemical Toxicology. 2022;4;45(3):963-71.
4. Elmarzugi NA, Keleb EI, Mohamed AT, Issa YS, Hamza AM, Layla AA, Salama M, Bentaleb AM. The relation between sunscreen and skin pathochanges mini review. International Journal of Pharmaceutical Science Invention. 2013;2(7):43-52.
5. Nemade H, Acharya A, Chaudhari U, Nembo E, Nguemo F, Riet N, Abken H, Hescheler J, Papadopoulos S, Sachinidis A. Cyclooxygenases inhibitors efficiently induce cardiomyogenesis in human pluripotent stem cells. Cells. 2020;27;9(3):554.
6. Kumaravel P, Melchias G, Vasanth N, Manivasagam T. Epigallocatechin gallate attenuates behavioral defects in sodium valproate induced autism rat model. Research Journal of Pharmacy and Technology. 2017;10(5):1477-80.
7. Yan HF, Tuo QZ, Yin QZ, Lei P. The pathological role of ferroptosis in ischemia/reperfusion-related injury. Zoological research. 2020;5;41(3):220.
8. Chen HS, Cui Y, Zhou ZH, Zhang H, Wang LX, Wang WZ, Shen LY, Guo LY, Wang EQ, Wang RX, Han J. Dual antiplatelet therapy vs alteplase for patients with minor nondisabling acute ischemic stroke: the ARAMIS randomized clinical trial. Jama. 2023;27;329(24):2135-44.
9. Jeelani SM, Rather GA, Sharma A, Lattoo SK. In perspective: Potential medicinal plant resources of Kashmir Himalayas, their domestication and cultivation for commercial exploitation. Journal of applied research on medicinal and aromatic plants. 2018;1;8:10-25.
10. Karthikeyan G, Vidya AK. Phytochemical analysis, antioxidant and antibacterial activity of pomegranate peel. Res. J. Life Sci. Bioinform. Pharm. Chem. Sci. 2019;5(1):218.
11. Abubakar AR, Haque M. Preparation of medicinal plants: Basic extraction and fractionation procedures for experimental purposes. Journal of pharmacy & bioallied sciences. 2020;12(1):1.
12. Fattepur S, Malik MZ, Nilual K, Abdullah I, Yusuf E, Asmani MF, Fatima MA, Kaleemullah M. Acute toxicity and antifungal activity of Pereskia bleo leaves extracts against Aspergillu. niger and Candida albicans. International Journal of Medical Toxicology & Legal Medicine. 2020;23(1and2):133-7.
13. Nagar HK, Srivastava AK, Srivastava R, Kurmi ML, Chandel HS, Ranawat MS. Pharmacological investigation of the wound healing activity of Cestrum nocturnum (L.) ointment in Wistar albino rats. Journal of Pharmaceutics. 2016;2016.
14. Shrivastav A, Mishra AK, Abid M, Ahmad A, Fabuzinadah M, Khan NA. Extracts of Tridax procumbens linn leaves causes wound healing in diabetic and Non-diabetic laboratory animals. Wound Medicine. 2020;1;29:100185.
15. Ali A, Garg P, Goyal R, Kaur G, Li X, Negi P, Valis M, Kuca K, Kulshrestha S. A novel herbal hydrogel formulation of moringa oleifera for wound healing. Plants. 2020;24;10(1):25.
16. Patil MV, Kandhare AD, Bhise SD. Pharmacological evaluation of ethanolic extract of Daucus carota Linn root formulated cream

on wound healing using excision and incision wound model. Asian Pacific Journal of Tropical Biomedicine. 2012;1;2(2):S646-55.
17. Murti K, Kumar U. Enhancement of wound healing with roots of Ficus racemosa L. in albino rats. Asian Pacific journal of tropical biomedicine. 2012;1;2(4):276-80.
18. Shrivastav A, Mishra AK, Ali SS, Ahmad A, Abuzinadah MF, Khan NA. In vivo models for assesment of wound healing potential: A systematic review. Wound medicine. 2018;1;20:43-53.
19. Ilango K, Chitra V. Wound healing and anti-oxidant activities of the fruit pulp of Limonia acidissima Linn (Rutaceae) in rats. Tropical Journal of Pharmaceutical Research. 2010;9(3).
20. Hastings J, Degtyarenko K, de Matos P, Ennis M, Steinbeck C. The ChEBI Ontology: An Ontology for Chemistry within a Biological Context. InSWAT4LS 2008.
21. Hastings J, Owen G, Dekker A, Ennis M, Kale N, Muthukrishnan V, Turner S, Swainston N, Mendes P, Steinbeck C. ChEBI in 2016: Improved services and an expanding collection of metabolites. Nucleic acids research. 2016;4;44(D1):D1214-9.
22. Havranek B, Islam SM. An in silico approach for identification of novel inhibitors as potential therapeutics targeting COVID-19 main protease. Journal of Biomolecular Structure and Dynamics. 2021;13;39(12):4304-15.
23. Mohammad T, Shamsi A, Anwar S, Umair M, Hussain A, Rehman MT, AlAjmi MF, Islam A, Hassan MI. Identification of high-affinity inhibitors of SARS-CoV-2 main protease: Towards the development of effective COVID-19 therapy. Virus research. 2020;15;288:198102.
24. Qureshi S, Khandelwal R, Madhavi M, Khurana N, Gupta N, Choudhary SK, Suresh RA, Hazarika L, Srija CD, Sharma K, Hindala MR. A multi-target drug designing for BTK, MMP9, proteasome and TAK1 for the clinical treatment of mantle cell lymphoma. Current Topics in Medicinal Chemistry. 2021;1;21(9):790-818.
25. Rai, H., Barik, A., Singh, Y.P., Suresh, A., Singh, L., Singh, G., Nayak, U.Y., Dubey, V.K. and Modi, G., 2021. Molecular docking, binding mode analysis, molecular dynamics, and prediction of ADMET/toxicity properties of selective potential antiviral agents against SARS-CoV-2 main protease: an effort toward drug repurposing to combat COVID-19. Molecular Diversity, 2021;25;1905-1927.
26. Shi T, Yang Y, Huang S, Chen L, Kuang Z, Heng Y, Mei H. Molecular image-based convolutional neural network for the prediction of ADMET properties. Chemometrics and Intelligent Laboratory Systems. 2019;15;194:103853.
27. Yang H, Lou C, Sun L, Li J, Cai Y, Wang Z, Li W, Liu G, Tang Y. admetSAR 2.0: web-service for prediction and optimization of chemical ADMET properties. Bioinformatics. 2019;15;35(6):1067-9.
28. Norinder U. C. a. S. Bergström. ChemMedChem. 2006;1:920-37.
29. Tuli HS, Bhatia GK, Sood S, Debnath P, Aggarwal D, Upadhyay SK. In silico analysis and molecular docking studies of plumbagin and piperine ligands as potential inhibitors of alpha-glucosidase receptor. Biointerface Res. Appl. Chem. 2020;11:9629-37.
30. Prasanth DS, Murahari M, Chandramohan V, Panda SP, Atmakuri LR, Guntupalli C. In silico identification of potential inhibitors from Cinnamon against main protease and spike glycoprotein of SARS CoV-2. Journal of Biomolecular Structure and Dynamics. 2021;2;39(13):4618-32.
31. Prasanth DS, Panda SP, Rao AL, Chakravarti G, Teja N, Vani VB, Sandhya T. In-silico strategies of some selected phytoconstituents from zingiber officinale as sars cov-2 main protease (COVID-19) inhibitors. Indian J Pharm Educ Res. 2020;1;54:s552-9.
32. Biovia DS. BIOVIA Discovery Studio Visualizer, v16. 1.0. 15350. San Diego: Dassault Systèmes. 2015;627:628.
33. Biovia DS. BIOVIA Discovery Studio Visualizer, v16. 1.0. 15350. San Diego: Dassault Systèmes. 2015;627:628.
34. Muralikrishnan A, Nair RR, Banu J, Pappachen LK. In silico designing of some Benzimidazole derivatives for Anti-fungal activity. Research Journal of Pharmacy and Technology. 2021;14(9):4983-6.
35. Wang Z, Li X, Chen H, Han L, Ji X, Wang Q, Wei L, Miao Y, Wang J, Mao J, Zhang Z. Decreased HLF expression predicts poor survival in lung adenocarcinoma. Medical Science Monitor: International Medical Journal of Experimental and Clinical Research. 2021
36. Ontoria-Oviedo I, Palacios I, Panadero J, Sánchez B, García-García F, López-Cerdán A, Dorronsoro A, Castellano D, Rodríguez-Borlado L, Bernad A, Sepúlveda P. Plasmatic membrane expression of adhesion molecules in human cardiac progenitor/stem cells might explain their superior cell engraftment after cell transplantation. Stem Cells International. 2020;10;2020.
37. Ontoria-Oviedo I, Palacios I, Panadero J, Sánchez B, García-García F, López-Cerdán A, Dorronsoro A, Castellano D, Rodríguez-Borlado L, Bernad A, Sepúlveda P. Plasmatic membrane expression of adhesion molecules in human cardiac progenitor/stem cells might explain their superior cell engraftment after cell transplantation. Stem Cells International. 2020;10;2020.
38. Patil VS, Hupparage VB, Malgi AP, Deshpande SH, Patil SA, Mallapur SP. Dual inhibition of COVID-19 spike glycoprotein and main protease 3CLpro by Withanone from Withania somnifera. Chinese Herbal Medicines. 2021;1;13(3):359-69.
39. Li X, Chen L, Cheng F, Wu Z, Bian H, Xu C, Li W, Liu G, Shen X, Tang Y. In silico prediction of chemical acute oral toxicity using multi-classification methods. Journal of chemical information and modeling. 2014;28;54(4):1061-9.